Journal of Physics: Conference Series **97** (2008) 012277 doi:10.1088/1742-6596/97/1/012277

Transmission electron microscopy analysis of C_4H_4S-doped MgB_2 tapes

N Yuzuriha[1], H Sosiati[2, 3], S Hata[1], N Kuwano[2], H Yamada[4], N Uchiyama[4], A Matsumoto[5], H Kitaguchi[5] and H Kumakura[5]

[1]Interdisciplinary Graduate School of Engineering Sciences, Kyushu University, Kasuga, Fukuoka 816-8580, Japan, [2]Art, Science and Technology Center for Cooperative Research, Kyushu University, Kasuga, Fukuoka 816-8580, Japan, [3]Research Laboratory for High Voltage Electron Microscopy, Kyushu University, Fukuoka 819-0395, Japan, [4]General Technology Division, Central Japan Railway Company, Komaki, Aichi 485-0801, Japan, and [5]National Institute for Materials Science, Tsukuba, Ibaraki 305-0047, Japan

E-mail: yuzurin6@asem.kyushu-u.ac.jp

Abstract. It has been reported that doping with aromatic hydrocarbons in an *in situ* powder-in-tube fabrication process of MgB_2 tapes is effective for increasing the critical current density (J_c) under magnetic fields. In this study, the mechanism of the J_c enhancement by doping with C_4H_4S was investigated by transmission electron microscopy (TEM). The C_4H_4S-doped MgB_2 tape has a denser cross-sectional microstructure than that of a non-doped MgB_2 tape. Electron diffraction and dark-field TEM observation indicated that the grains of MgB_2 are well crystallized and slightly increase in size with the C_4H_4S doping. X-ray diffraction and two-dimensional elemental mapping using characteristic x-rays suggested that C atoms substitute part of B atoms in MgB_2 crystals. Unlike other kinds of impurity doping, such as SiC-doping, there were few nanosized inclusions formed by C_4H_4S doping. Thus, it is concluded that the J_c enhancement with the C_4H_4S doping is due to (i) increasing supercurrent and magnetic-flux pinning at grain boundaries by the formation of dense and well-crystallized MgB_2 matrix and (ii) increasing the upper critical field by the formation of $Mg(B,C)_2$.

Introduction

MgB_2 is a superconductor showing the high critical temperature (39 K) [1] in comparison with other metallic superconductors. Furthermore, the low cost of the raw materials, Mg and B, attracts attention from the practical point of view. Therefore, MgB_2 is expected as a superconducting material in the next generation. However, the critical current density (J_c) drops rapidly in a magnetic field. This is a current disadvantage of MgB_2 for practical use. Since the J_c is sensitive to microstructure, various kinds of fabrication processes for MgB_2 materials have been reported to improve J_c properties. In the case of tapes, various additives and processing conditions are studied to increase J_c as well as the upper critical field (H_{c2}). It is known that a significant increase of J_c under magnetic fields is achieved by adding nanosized SiC powder in an *in situ* process [2-9]. It is thought that one of the reasons of the J_c enhancement by SiC doping is substitution of C atoms for B sites in MgB_2 crystals [2-8, 10]. Several C sources have shown positive effects on J_c and H_{c2} [11, 12]. It has been found that addition of

aromatic hydrocarbons is very effective for increasing J_c under magnetic fields [13]. For example, the J_c values in MgB_2 tapes doped with thiophene (C_4H_4S) are almost equal to those in SiC-doped MgB_2 tapes. However, the mechanism of the significant J_c enhancement by doping with C_4H_4S is not clear because of the lack of detailed microstructure analysis.

In this study, microstructures in a C_4H_4S-doped MgB_2 tape fabricated by an *in situ* powder-in-tube (PIT) process are investigated using transmission electron microscopy (TEM) techniques. Three other MgB_2 tapes fabricated by different *in situ* PIT processes are also investigated for comparison: a non-doped MgB_2 tape, an SiC-doped MgB_2 tape and an MgB_2 tape fabricated with a ball-milling treatment of starting materials. Based on microstructural features of these MgB_2 tapes, the effect of C_4H_4S doping will be discussed.

1. Experimental details

An MgB_2 tape doped with C_4H_4S was prepared by the following fabrication steps: step 1, commercial MgH_2 and amorphous B powders were mixed with the nominal composition of 1:2 (MgB_2); step 2, 20 mol% C_4H_4S was added into the mixed powder; step 3, the mixed powders were well mixed using a ball-milling method under a high-purity argon gas atmosphere; step 4, the mixed powder was packed into pure Fe tube with the inner and outer diameters 4 and 6 mm, respectively; step 5, the MgB_2/Fe tube was cold-rolled into a tape 4 mm width and 0.5 mm thickness by groove rolling and flat rolling; step 6, the obtained MgB_2/Fe tape was heated up to 600°C in 0.5 h, kept at 600°C for 1 h and then cooled down to room temperature in a furnace. For a non-doped MgB_2 tape, steps 2 and 3 were skipped. For an SiC-doped MgB_2 tape, 10 mol% of nanosized SiC powder was added instead of C_4H_4S in step 2 and mixed with the MgH_2 and B powders by hand milling in step 3. For a ball-milled MgB_2 tape, commercial Mg powder was used instead of the MgH_2 powder in step 1 and step 2 was skipped.
The transport critical current (I_c) in the prepared MgB_2/Fe tapes was measured by a standard four-probe resistive method in a magnetic field at 4.2 K. The criterion of I_c definition was 1 μVcm^{-1}. The magnetic field was applied parallel to the main plane of the tapes.

Powdered samples were picked up from the core of the MgB_2/Fe tapes, and crystalline phases formed in the samples were identified by conventional X-ray diffraction (XRD) experiments (PHILIPS PW-1730) using the θ-2θ method.

Overall microstructures were observed in polished cross-sections of the MgB_2/Fe tapes using a

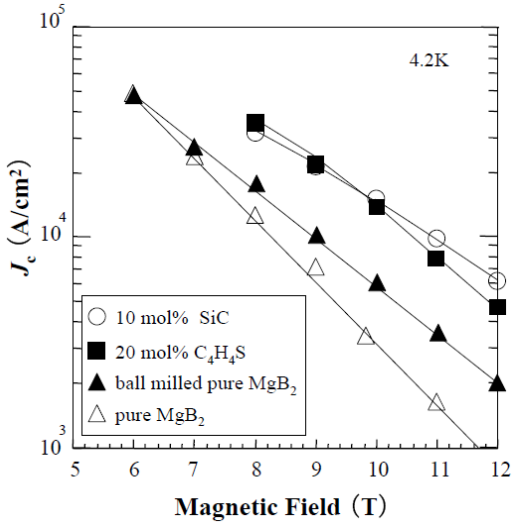

Figure 1. J_c as a function of the magnetic field.

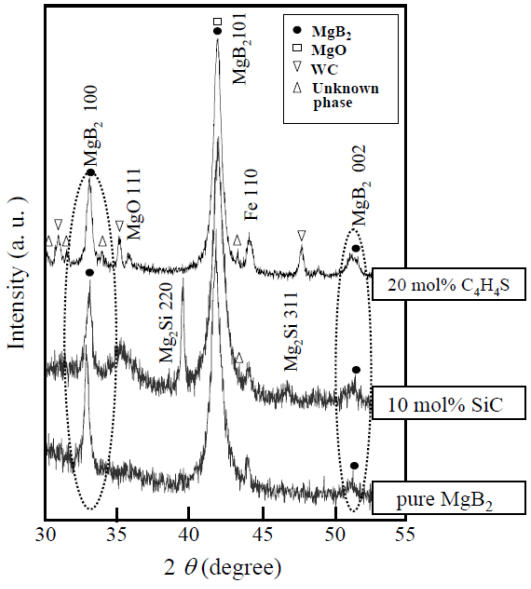

Figure 2. X-ray diffraction patterns.

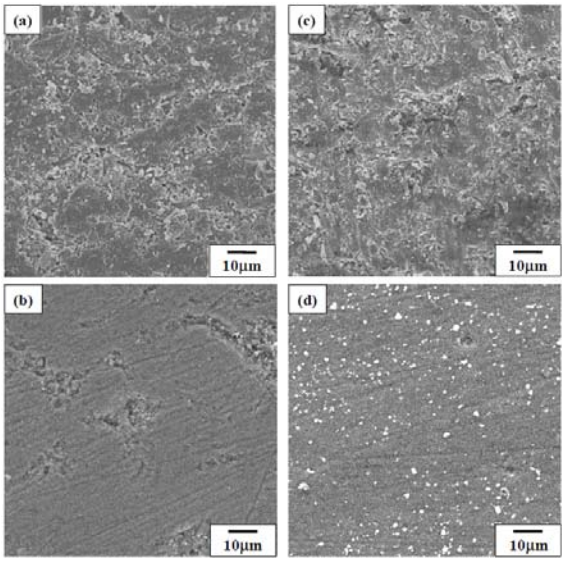

Figure 3. Cross-sectional SEM images of pure MgB_2 (a), ball-milling tape (b), SiC-doped tape (c) and C_4H_4S-doped tape (d).

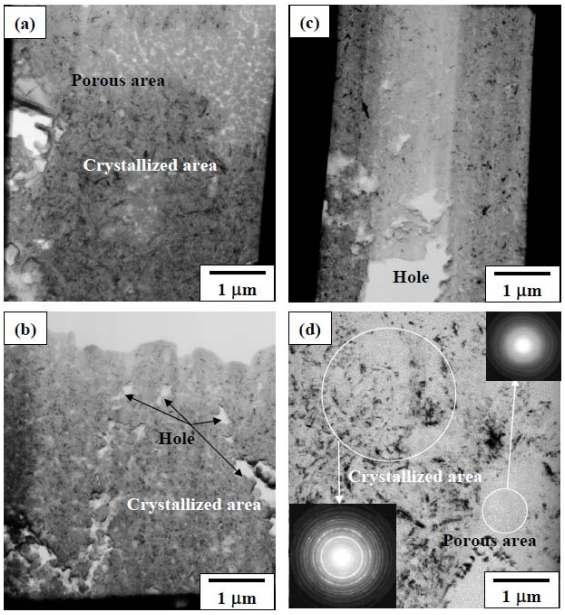

Figure 4. Bright-field TEM images and corresponding diffraction patterns of pure MgB_2 (a), ball-milling tape (b), SiC-doped tape (c) and C_4H_4S-doped tape (d).

JEOL JSM-6340F scanning electron microscope (SEM). Thin foil specimens were picked up from the cross-sections using a focused ion beam (FIB) microsampling technique. The accelerating voltage of the FIB mill (HITACHI FB-2000K) was 30 kV and final specimen thicknesses were 150-200 nm to keep non-damaged regions after Ga^+ ion milling. Before TEM experiments, an Ar-plasma treatment was carried out to prevent contaminations on the specimen surface.

Detailed microstructure characterizations were performed using an FEI TECNAI-F20 transmission electron microscope (TEM) equipped with scanning TEM (STEM) and energy dispersive x-ray spectroscopy (EDXS) systems. In addition to conventional observations, two-dimensional elemental mapping was carried out by a combination of the STEM and EDXS techniques. In the STEM-EDXS elemental mapping, the electron beam about 1 nm in diameter was positioned on the specimen surface, and an EDX spectrum was acquired for 4 s at each position. Elemental maps were obtained by displaying integrated intensities of characteristic x-rays (B K: 0.18 keV, C K: 0.28 keV, O K: 0.53 keV, Mg K: 1.25 keV, S K: 2.30 keV) at each of the acquisition points without background subtraction.

2. Result and discussion

2.1. J_c properties

Figure 1 shows J_c values in the fabricated MgB_2 tapes measured as a function of the magnetic field. The J_c value of the C_4H_4S-doped tape was 1.3×10^4 A/cm^2 at 10T. The J_c values of the C_4H_4S-doped tape were much higher than that of pure MgB_2 tape below all magnetic fields and much higher than that of SiC-doped tape less than 8T.

Compared with ball-milling tape, the J_c values of C_4H_4S-doped tape were much higher than that of ball-milling tape. However, the slope of J_c dependence of C_4H_4S-doped tape is much higher than that of ball-milling tape. The slope of J_c dependence being high means that the flux pinning is not enhanced. Therefore, the flux pinning of C_4H_4S-doped tape was not enhanced compared with ball-milling tape and SiC-doped tape.

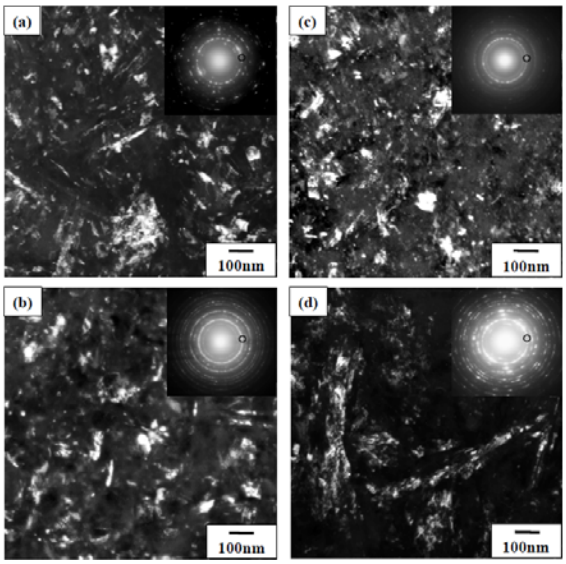

Figure 5. Low-magnification bright-field TEM images and corresponding diffraction patterns of pure MgB_2 (a), ball-milling tape (b), SiC-doped tape (c) and C_4H_4S-doped tape (d).

2.2 X-Ray diffraction patterns

Figure 2 shows the XRD patterns of the fabricated tapes. In the C_4H_4S-doped tape, the main phase is MgB_2 and Fe, MgO, and WC as impurity phases. The diffraction peaks from Fe are due to mixing of the Fe sheath material in the specimen preparation and WC are due to mixing during ball mill method. In addition, some unidentified small peaks were seen. MgB_2 peaks of C_4H_4S-doped tape were sharp and strong, compared with that of other tapes. It indicates that MgB_2 crystallizes, and MgB_2 crystal grains grow up greatly. In addition, 100 hkl = diffraction peaks of MgB_2 observed at 2θ= 33-34 degrees slightly shift to the high angle side in comparison with the pure MgB_2 tape. In other words, the a-axis length of the MgB_2 crystal lattice was shrunk. This tendency suggests that C atoms substitute it for one part of the B atoms of a MgB_2 crystal [10].

2.3. Cross sectional SEM

Figure 3 shows a cross sectional SEM images of the fabricated tapes. In comparison with the pure MgB_2 tape, the C_4H_4S-doped tape had few voids and cracks with a dense organization. This accords with a characteristic to be seen in the organization of ball-milling tape. On the other hand, the organization of SiC-doped tape does not almost change with pure MgB_2 tape. Therefore, an associativity of MgB_2 improves by doping of C_4H_4S and ball-milling method. The white impurities seen in the surface of C_4H_4S-doped tape are SiC which got mixed because SiC uses Emery paper of the abrasive when thinning and polished tape.

2.4. TEM analysis

Figure 4 shows bright-field TEM low magnification image of the fabricated tapes. The thinning area consists of a crystallized area with dark contrast, the area without the contrast and the area of the hole. In the C_4H_4S-doped tape, the electron diffraction pattern taken from dark contrast area can confirm a lot of debye rings and a diffraction spot showing polycrystalline of MgB_2 and MgO. The completeness of a crystal of MgB_2 was high from electron diffraction patterns. On the other hand, in electron diffraction pattern taken from the area without the contrast can confirm halo patterns to show the existence of the amorphous substance phase. The area without the contrast to show these amorphous substances were seen a lot around holes. The dense MgB_2 areas were seen a lot, compared with pure

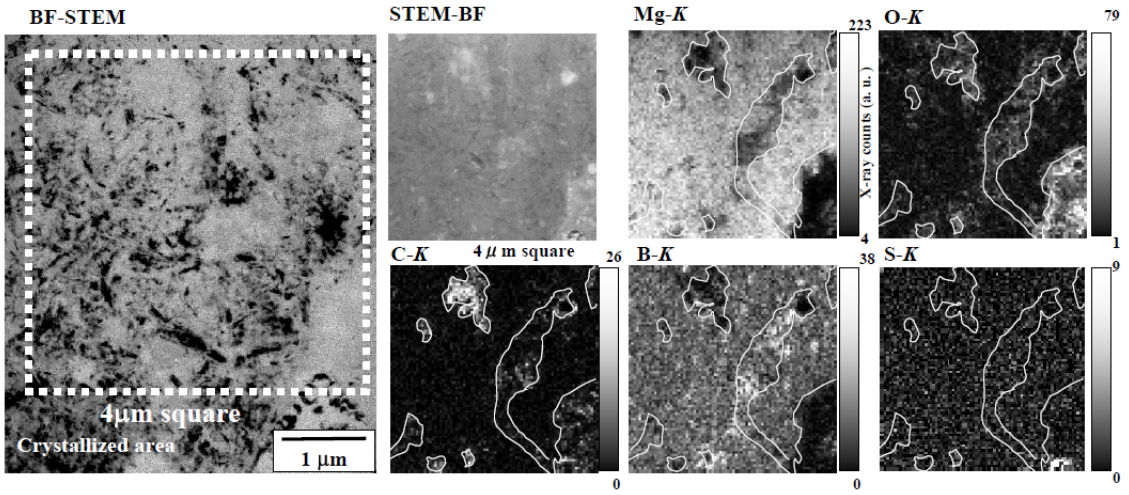

Figure 6. Low magnification STEM Bright-field image and EDS elemental maps in C_4H_4S-doped MgB_2 tapes.

MgB_2 tape, and the number of small holes were less, compared with other tapes. This indicated that minute MgB_2 were formed by C_4H_4S.

2.5. STEM-EDXS analysis

Figure 5 shows a STEM-EDXS elemental mapping result of low magnification for C_4H_4S-doped tape. The elemental mapping was performed in a square of dashed line 4μm mapping area. The O-rich areas were shown the white lines in all elemental maps. The O map shows a lot of O atoms exist nearly porous areas and showed the distribution that resembled B and C of high density. This tendency indicated that remaining C (amorphous substance or graphite) which was not taken in by MgB_2 or C that C_4H_4S is carbonized by heat-treatment adsorbed O. The detailed distribution of S tendency was not seen because there is few count number of S.

Figure 6 shows an elemental mapping result for C_4H_4S-doped tape. The elemental mapping was performed in a square of dashed line 150nm mapping area. The O-rich areas were shown the white lines in all elemental maps. C atoms show a tendency to be distributed in a MgB_2 matrix uniformly, and some C atoms substitute it for B atoms of the MgB_2 crystal [2, 4-8]. It accords with XRD experiment. The distributions of O were partly similar to that of Mg. This indicated that MgO was formed. There was the distribution that resembled S and C partly.

The element mapping of pure MgB_2 tape and SiC-doped tape are already reported [14], and, in the pure MgB_2 tape, there is MgO in the border of a crystallization area and non-crystallization area locally. In the SiC-doped tape, C is distributed in a MgB_2 matrix uniformly and some Si forms Mg_2Si. The element distribution of C_4H_4S-doped tape resembled it with distribution of SiC-doped tape. In addition, it resembled C_4H_4S-doped tapes with SiC-doped tapes to be effective in scattering MgO uniformly.

3. Conclusion

It is effective for increase J_c to add C_4H_4S in initial powders. The value of J_c is comparable to that of SiC-doped tape. The microstructure of C_4H_4S-doped tape had both parts of a characteristic of ball-milling tape and SiC-doped tape. A section organization of tapes resembled ball-milling tape and was dense. The completeness of a crystal of MgB_2 was high from electron diffraction patterns. But the size of a MgB_2 crystal of C_4H_4S-doped tape increased a little. This is different from ball-milling tape and SiC-doped tape. C was distributed of a MgB_2 matrix uniformly. Same as SiC-doped tape, it is thought that C atoms substitute it for one part of the B atoms of a MgB_2 crystal. Unlike SiC-doped tape, there

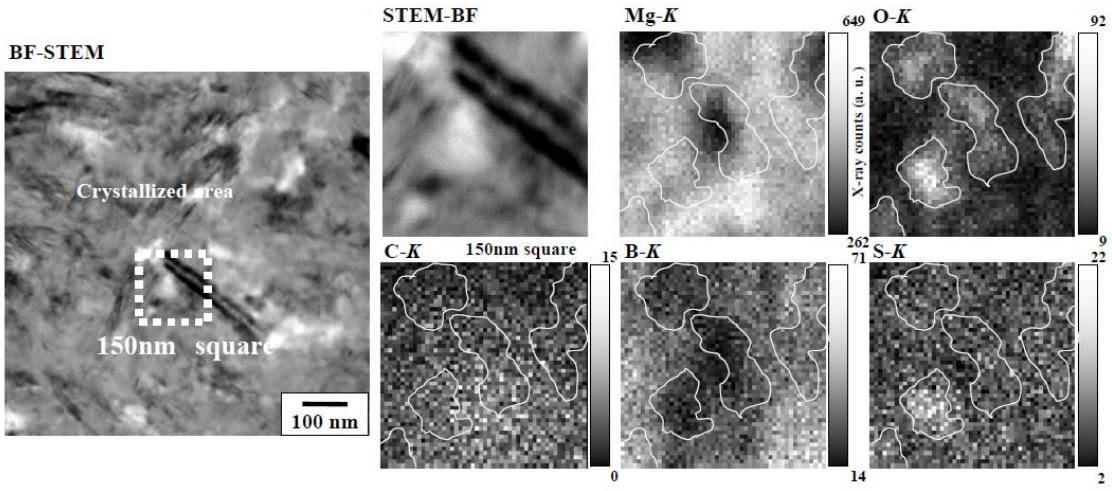

Figure 7. STEM Bright-field image and EDS elemental maps in C_4H_4S-doped MgB_2 tapes.

were very few minute impurities based on C and S in C_4H_4S-doped tape. It is thought that it contributes to raising the formation of the above-mentioned dense, high MgB_2 crystal and associativity between MgB_2 crystal grains that minute impurities are very small amounts. In addition, it is considered when improvement of J_c in a high magnetic field side is caused by rise of upper critical field with the formation of $Mg(B,C)_2$ and flux pinning by MgB_2 crystal grain boundary mainly [2,5,6,9].

Acknowledgments

This work was supported in part by Nanotechnology Support Project of the Ministry of Education, Culture, Sports, Science and Technology (MEXT), Japan.

References

[1] Nagamatsu J, Nakagawa N, Muranaka T, Zenitani Y and Akimitsu J 2001 *Nature* **410** 63-4.
[2] Dou S X, Soltanian S, Horvat J, Wang X L, Zhou S H, Ionescu M, Liu H K, Munroe P and Tomsic M 2002 *Appl. Phys. Lett.* **81** 3419-21.
[3] Wang X L, Yao Q W, Horvat J, Qin M J and Dou S X 2004 *Supercond. Sci. Technol.* **17** L21-4.
[4] Wang X L, Soltanian S, James M, Qin M J, Horvat J, Yao Q W, Liu H K and Dou S X 2004 *Physica C* **408-410** 63.
[5] Dou S X, Braccini V, Soltanian S, Klie R, Zhu Y, Li S, Wang X L and Larbalestier D 2004 *J. Appl. Phys.* **96** 7549-55.
[6] Soltanian S, Wang X L, Hovart J, Dou S X, Sumption M D, Bhatia M, Collings E W, Monroe P and Tomsic M 2005 *Supercond. Sci. Technol.* **18** 658.
[7] Dou S X, Yeoh W K, Horvat J and Ionescu M 2003 *Appl. Phys. Lett.* **83** 4996.
[8] Cava R J, Zandbergen H W and Inumaru K 2003 *Physica C* **385** 8.
[9] Kumakura H, Kitaguchi H, Matsumoto A and Hatakeyama H 2004 *Appl. Phys. Lett.* **84** 3669.
[10] Kumakura H, Kitaguchi H, Matumoto A and Yamada H 2005 *Supercond. Sci. Technol.* **18** 1042.
[11] Wang X L, Yao Q W, Horvat J, Qin M J and Dou S X 2004 *Supercond. Sci. Technol.* **17** L21.
[12] Ma Y, Kumakura H, Matsumoto A, Hatakeyama H and Togano K 2003 *Supercond. Sci. Technol.* **16** 852.
[13] Yamada H, Hirakawa M, Kumakura H and Kitaguchi H 2006 *Supercond. Sci. Technol.,* **19** 175-177.
[14] Hata S, Yoshidome T, Sosiati H, Tomokiyo Y, Kuwano N, Matsumoto A, Kitaguchi H and Kumakura H 2006 *Supercond. Sci. Technol.* **19** 161-168.